Tuning the properties of two-dimensional materials by atomic scale structural defects

OTKA KH130413 (2018-2020)

-Final Scientific Report-

In this two-year OTKA project we have investigated the effect of atomic scale structural defects on the properties of two-dimensional (2D) materials, also focusing on the possibilities for tuning these properties for specific applications. Until the end of the project 7 publications have appeared with a total impact of 48.5. At the time of writing, further manuscripts are prepared for publications. In the following, we will present our main results, which can be classified into three main areas:

1) Defect engineering of electronic and magnetic properties
2) Effect of defects on the catalytic activity
3) Tuning the optical properties with defects

The publications, where further detailed of the results can be found, is given in the list of publications belonging to this final report.

Defect engineering of electronic and magnetic properties

The possibility to modify the electronic properties of 2D materials with defects have been demonstrated by us before the start of the project in the case of sulfur vacancies in MoS_2. These results have motivated the present project to combine electronic structure calculations and atomic resolution Scanning Tunneling Microscopy (STM) and tunneling spectroscopy (STS) measurements in order to predict the impact of various point and line defects in different 2D materials.

Defects in CVD grown 2D $MoSe_2$

We have investigated experimentally and theoretically the properties of CVD grown $MoSe_2$ single-layers on graphite. By using STM, we have observed the rotationally aligned growth of $MoSe_2$ single layers and a reduced grain boundary (GB) density compared to samples grown by Molecular Beam Epitaxy (MBE). Due to the rotationally aligned growth, these GBs are predominantly mirror twin boundaries (MTBs) running along the zigzag direction of the lattice, as revealed by atomic resolution STM images (Fig. 1a). We used DFT calculations to reveal the atomic and electronic structure of the observed line defects (MTBs). We have found that in contrast to other types of grain boundaries, MTBs along zigzag directions do not induce

considerable structural or electronic modifications of the pristine crystal, only minor perturbations are visible inside the band gap due to localized metallic states at the boundary. The hallmark of these metallic states was also observed in the experiments. These findings can open the way towards the CVD growth of large-area $MoSe_2$ single layers of high structural and electronic quality. Besides the revealed line defects in $MoSe_2$, point defects were also observed, identified as Mo vacancies (Fig. 1b-c).

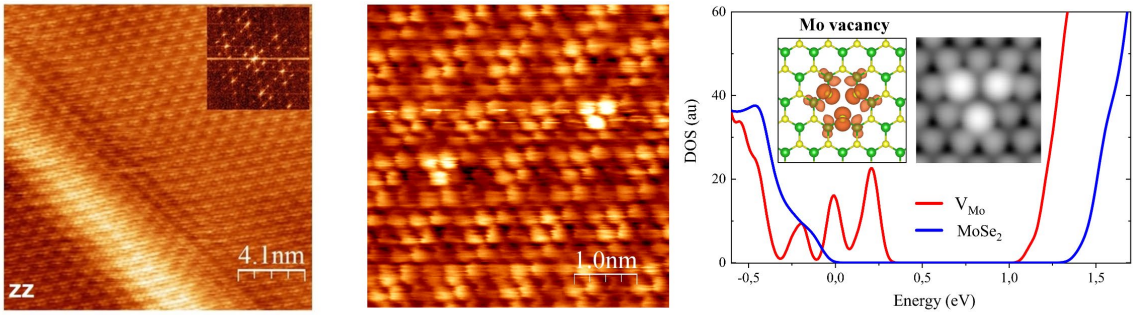

Figure 1. Atomic resolution STM images of native point defects in $MoSe_2$ single layers. (a) MTB running along the zigzag crystallographic orientation (b) Mo vacancy. (c) Calculated LDOS of the Mo vacancy. The inset shows isosurface plot of the spin density and the simulated STM image of the Mo vacancy.

According to the DFT calculations these vacancies significantly reduce the bandgap of $MoSe_2$ and also host localized magnetic moments, which can be electrically controlled by tuning the Fermi level between 0 and 5 μ_B values. Our results show that through Mo vacancies it is possible to realize an efficient electrical control of the magnetism in 2D $MoSe_2$ crystals. The results have been published in Journal of Physical Chemistry C.

Magnetic properties of the zigzag edges in MoS_2

The properties of the edges of 2D materials (one-dimensional defects) usually significantly differ from the bulk (basal plane). In the case of MoS_2, previous studies have revealed ferromagnetic and metallic behavior of the edges having zigzag orientation; however, the computational costs of the *ab initio* methods restrict the calculations to small systems. In the present project we decided to perform large-scale calculations by using tight-binding (TB) and Hubbard Hamiltonians to reveal the magnetic properties of edges with realistic disorder scales. As a first step, we demonstrated that the metallic states of zigzag MoS_2 nanoribbons can be reproduced with their proper orbital characters by adapting TB parameters for the edge atoms. These results provided us a good starting point for further inclusion of the electron-electron interactions, where the Coulomb repulsion was taken into account by using local Hubbard interaction terms in the fine-tuned TB Hamiltonian. Our results show that despite of the large magnetic moments (0.35 μ_B on the S atoms at the S edge) the spins are weakly coupled along

the edge. The calculated collinear domain-wall creation energy in a 13 nm long edge is only +6.5 meV, which is more than 1 order of magnitude lower compared to the case of zigzag graphene nanoribbons.

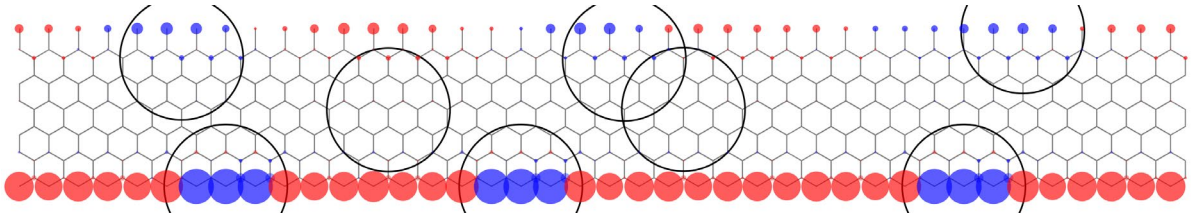

Figure 2. Calculated magnetic ground state in the presence of disorder. Black circles denote the positions of the randomly distributed Gaussian potentials with V_0 =+100 meV. The radii of the circles correspond to the sizes of the potentials. Blue and red circles correspond to spin-up and spin-down electrons.

We also investigated short- and long-range disorders originating from inhomogeneous charge distribution of the substrate. We have predicted that the magnetic ground state strongly depends on the applied potential parameters, where even a disorder of a few atomic distances can change the orientation of the edge spins resulting domain-walls (Fig. 2). Apart from the particular interest of the results in the case of MoS_2, our approach of the magnetic calculations also opens the way for investigating electron-electron effects in other large-scale systems. The results have been published in Physical Review Materials.

Topological edge states in a novel quantum spin hall (QSH) material

Besides the well-known 2D materials (graphene, TMDC etc.) we also extended our investigations to other layered materials having peculiar properties. We demonstrated for the first time that layered mineral jacutingaite (Pt_2HgSe_3) is a candidate QSH material, where the helical locking of spin and momentum suppresses backscattering of charge carriers resulting in topological protected edge states. By using DFT calculations we obtained ~100 meV band gap of the monolayer and also confirmed the topological nature of the gap in excellent agreement with the STS measurements. During the STM investigation we observed that edges always follow the zigzag orientation of the lattice. Therefore, we performed detailed DFT electronic structure calculations of this edge orientation terminated by Se, Pt, and Hg, by optimizing the atomic lattice of monolayer ribbons. From comparing our calculations with experimental results, we were able to determine the experimentally observed edge configuration (Se terminated zigzag edge), which also has the lowest formation energy (Fig. 3). The calculated topological edge state shows the same atomic periodicity as observed in the measurements.

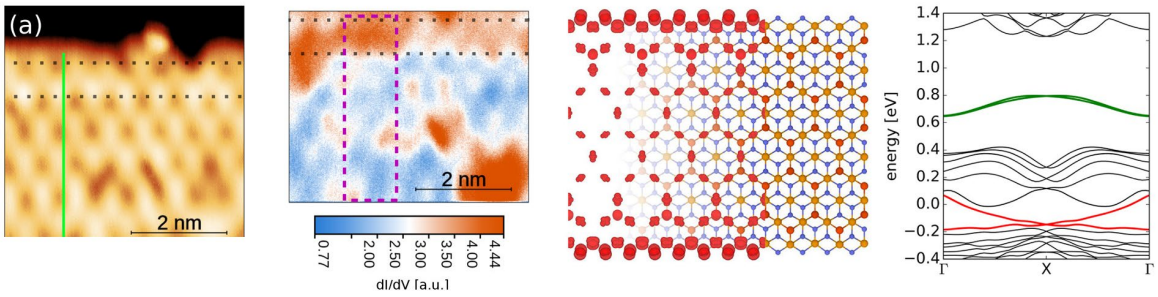

Figure 3. (a) Topography STM image of the zigzag edge (b) dI/dV image of the same area measured inside the gap. (c) Calculated LDOS of the topological edge state and (d) Band structure of the Se terminated zigzag ribbon, where the topological edge state marked by red curves.

The large band gap of the materials enables room temperature dissipation-free transport because the topological edge states is not perturbed by the presence of defects, as it is evidenced also in Fig. 3a. This property makes jacutingaite a promising material for applications from low-power electronics to quantum computing. The results have been published in Nano Letters.

Transport calculations by using wave packet dynamical method

Wave packet dynamics (WPD) can simulate electronic dynamics and transport phenomena at the nanoscale and it is capable to calculate realistic models containing several hundred atoms including also structural disorder. The WPD calculation has two input quantities, the Hamiltonian and the $\psi_0(\vec{r})$ initial state. In the project we have further developed our WPD code in two important directions: (i) preparing well defined $\psi_0(\vec{r})$ initial states constructed from the superposition of Bloch states (ii) incorporating the $E(\vec{k})$ dispersion relation directly into the kinetic energy operator of the Hamiltonian. Both developments are necessary if one would like to calculate accurate transport properties within WPD method for different 2D materials. The first development makes it possible to fine-tune the spectral distribution of the initial wave packet and thus we can prepare proper initial states for different scenarios, such as electrons injected from metallic electrode or electrons excited optically, etc. We applied the method for a structural defect on a graphene surface, where we studied the scattering of the Bloch function wave packet on the local defect and on defective graphene nanoribbons. In the second development, the properties of the infinite crystal (its atomic- and electronic structure) is coded into the kinetic energy operator and the properties of the defect is represented by a local potential. The advantage of the method is that we can extend the WPD calculations on any 2D materials by using the $E(\vec{k})$ band structure of crystal available from DFT calculations. We demonstrated the method on graphene with local disorder potential, where the scattered wavepacket has hexagonal symmetry. The results have been published in the conference

proceedings of the 1st International Electronic Conference on Applied Sciences (received the Best Paper Award) and in JETP Letters.

Effect of defects on the catalytic activity

In our previous work [J. Pető et al., Spontaneous doping of 2D MoS_2 basal plane by oxygen substitution during ambient exposure. Nat. Chem. 10, 1246 (2018)] we showed that oxygen atom substitution sites in MoS_2 are important point defects that increase the catalytic activity of the 2D crystals. During the present project, we have further investigated both theoretically and experimentally the relation between the modified defect properties and the catalytic activity.

Theoretical investigation of single atom catalysis in TMDs

We have performed detailed DFT calculations in six different TMD single-layers in order to investigate the effect of oxygen substitution. We especially focused on those physical properties, which can be related to the increased activity of the hydrogen evolution reaction (HER). First, we found that the Gibbs free energy of the H atom adsorption considerably decreases on the O substitution site, indicating a more favorable H atom adsorption on such O substitution sites than the pristine chalcogen atoms of the basal plane. Second, Bader charge analysis revealed significant charge transfer resulting in a negatively charged O atom due to the different electronegativity as compared to the substituted chalcogenide atoms. The partially screened negative charges can provide an additional attractive interaction for the positively charged H species facilitating their adsorption. Finally, the electronic structure calculations revealed increased transverse conductivity around the defect. Since the electrode is located right under the TMD layer in the electro-catalytic setup, the increased conductivity in the z-direction improves the electron transfer at the position of the oxygen sites required for efficient electrocatalytic reactions (Fig. 4). Overall, we conclude that the mentioned defect-modified properties are responsible together for the observed, substantially increased catalytic activity. The results have been published in ACS Energy Letters.

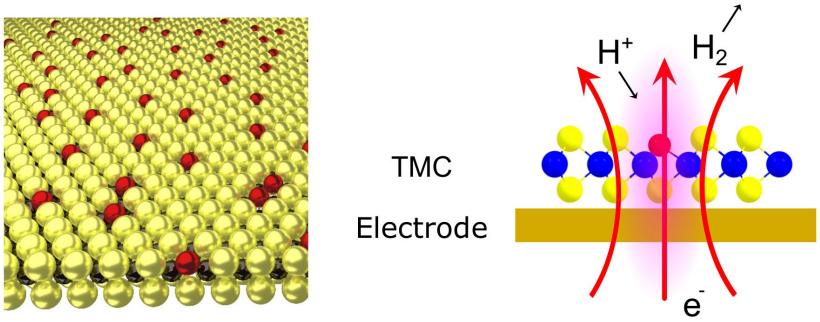

Figure 4. (a) Schematic model of individually dispersed heteroatoms substituting chalcogenide atoms of 2D TMD. (b) illustration of the HER mechanism.

Investigation of 2D $MoS_{2(1-x)}Se_{2x}$ solid solution crystals grown by CVD

The observed catalytic activity of the O substitution defect has turned our attention to other type of defects in MoS_2. The CVD method allows us to synthesize $MoS_{2(1-x)}Se_{2x}$ monolayer alloys in a controlled way, where, in the limit of low Se content, the incorporated Se atoms can be regarded as defects in the MoS_2 lattice. Therefore, we produced $MoS_{2(1-x)}Se_{2x}$ samples by using atmospheric pressure CVD, where different ratio of S and Se powders were evaporated during the growth. The synthesized samples were characterized with STM, Raman, XPS and Kelvin probe techniques. According to the measurements the CVD grown $MoS_{2(1-x)}Se_{2x}$ samples had different Se contents from x=0.05 to x=0.2. Our STM investigation revealed that Se atoms are not randomly distributed in the host lattice. We found Se rich regions forming larger triangular clusters (Fig. 5a) and also Se atoms incorporated along lines into the MoS_2 lattice (Fig. 5b). To investigate the catalytic activity of the grown $MoS_{2(1-x)}Se_{2x}$, electrochemical measurements for the hydrogen evolution reaction (HER) were performed. We found improved catalytic activity compared to the pristine MoS_2, however, no clear correlation was revealed between the catalytic activity and the Se content. The results indicate that not only the concentration of the Se content, but also the geometry of the incorporated Se atoms plays an important role in the catalytic performance, therefore the observed non-uniform Se distribution may also have an impact on the catalytic properties. Our findings can be useful for the investigation of catalytic effects in other 2D alloys. The manuscript is under preparation.

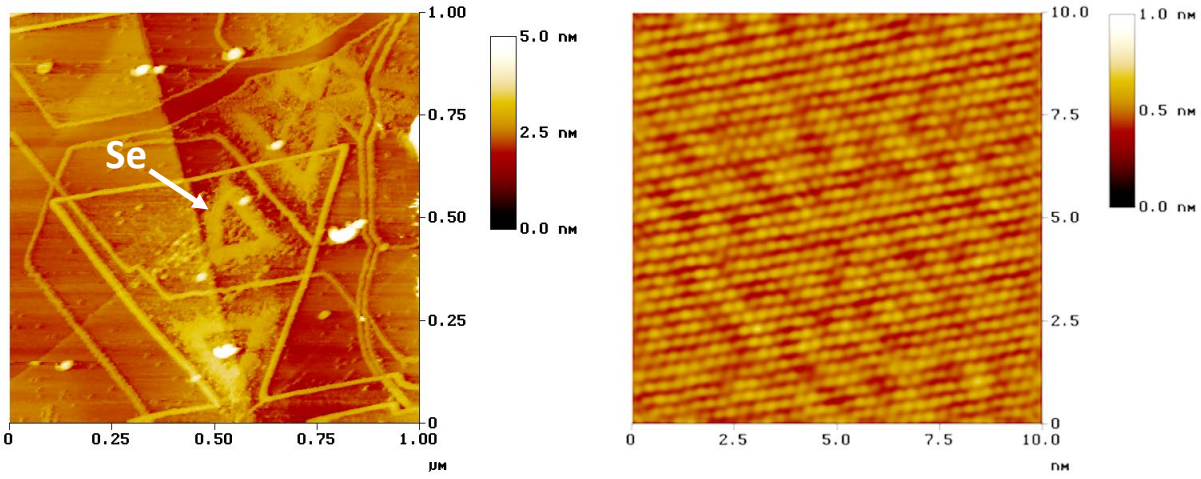

Figure 5. Topographic STM images of $MoS_{2(1-x)}Se_{2x}$. (a) Triangles with broadened edge contour corresponds to the Se rich regions. (b) Atomic resolution image shows contrast change along lines attributed to Se atoms.

Tuning the optical properties with defects

In the original work plan we proposed to investigate the optical properties of WSe_2 point defects, however due to rapid development of research in the field of 2D materials, this topic was mostly covered by others at the very beginning of the project. Instead, we studied the effect of strain (atomic lattice deformation) on the electronic and optical properties of MoS_2 and graphene.

Strain induces direct-indirect band gap transition in MoS_2

In MoS_2, nanobubbles characterized by a few percent of biaxial tensile strain have been investigated by STM measurements. The origin of such bubbles is the relatively strong Van der Waals interaction that squeezes the contaminants trapped at the MoS_2/Au(111) interface into nanoscale bubbles (Fig. 6a). By comparing the electronic and optical bandgaps of strained MoS_2 single layers obtained from tunneling spectroscopy and photoluminescence measurements, we found that upon 2% biaxial tensile strain, the electronic gap becomes significantly smaller (1.45 eV) than the optical direct gap (1.73 eV), clearly evidencing a direct-to-indirect band gap transition. Our DFT calculations also confirmed this transition to occur below 2% biaxial strain, where the valence and conduction bands near the K point downshift in energy, while the valence band position near the Γ point remains almost unaffected relative to the Fermi energy (Fig. 6b-c). The downshift near the K point can also explain the metallic behaviour observed in experiments considering the intrinsic n-doping of the material. The results have been published in npj 2D Materials and Applications.

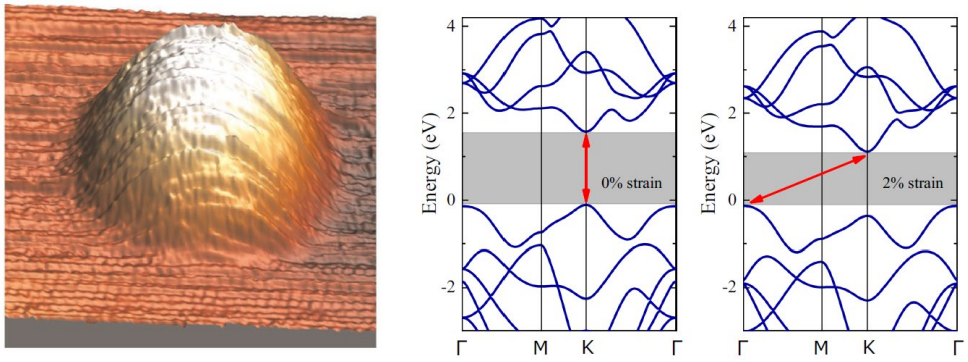

Figure 6. (a) 3D STM image of an individual MoS_2 nanobubble of 1 nm height and 10 nm diameter. (b-c) DFT calculated band structure of MoS_2 single layer for 0% and 2% biaxial tensile strain.

Optical excitations in graphene nanocorrugations

Graphene sheets with strong nanoscale corrugations were prepared by cyclic thermal annealing in our group. These nanocorrugated graphene samples show huge enhancement of the Raman

signals of adsorbed molecules (CuPc, ZnPc) clearly beyond the range of chemical enhancement. Within the present project, we have theoretically studied the electronic and optical properties of nanocorrugated graphene to understand the experimentally observed Raman enhancement mechanism. Our first-principles calculations revealed strong modification of the electron density of states and increased in-plane conductivity in the presence of the corrugation compared to quasi-flat sheets. These modifications enable localized plasmon excitations of energies in the visible range, according to the calculated electron energy loss (EELS) spectrum that directly reveals plasmon peaks (Fig. 7). From the plotted spatial charge distributions at the resonance frequencies, we can further analyze the properties of these excitations. For example, the mode at 1.9 eV has a dipolar character, localized around the top of the graphene protrusion (Fig. 7 inset). The predicted localized graphene plasmons at visible frequencies, obtained from the DFT calculations, support the plasmonic origin of the observed huge Raman enhancements in the measurements. The manuscript presenting the results has been sent out for external review in Nature Nanotechnology.

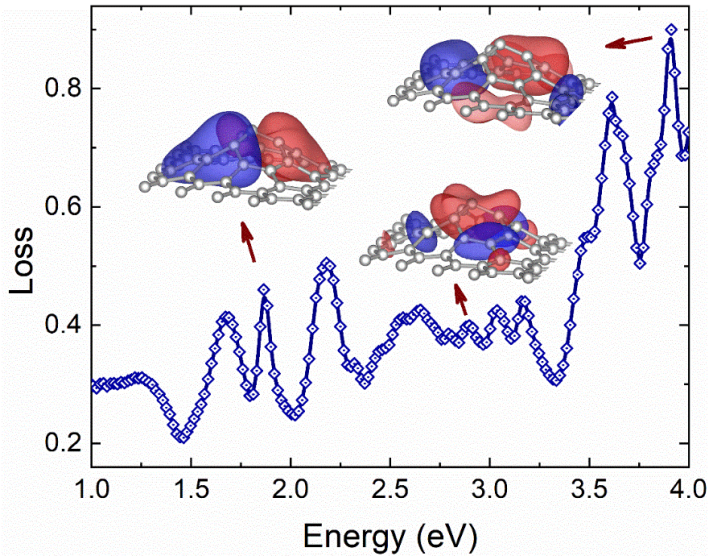

Figure 7. Calculated EELS spectrum of a model graphene nanocorrugation, revealing several loss peaks in the visible range. The insets display the charge distributions of plasmonic excitations corresponding to different loss peak near 1.9 eV, 2.9 eV, and 3.9 eV.

Finally, we note that the results of the present project were presented in several invited and oral presentations at international and national scientific conferences (>10). According to the recommendations of the final report, only those conference presentations are given in the publication list, which have not been published in scientific journals till the end of the project.